

1
2
3 **Title: Myocardial Blood Flow Reserve Is Impaired In Patients With Aortic Valve Calcification And**
4
5 **Unobstructed Epicardial Coronary Arteries**
6
7

8
9 Karen Nel¹, Michael C Y Nam², Chris Anstey³, Christopher J Boos⁴, Edward Carlton⁵, Roxy Senior⁶, Juan Carlos
10 Kaski⁷, Ahmed Khattab⁸, Delva Shamley⁹, Christopher Byrne¹⁰, Kim Greaves¹¹
11

12
13
14 ¹Department of Cardiology, Poole Hospital NHS Foundation Trust, Centre for Postgraduate Medical Research
15 and Education, Bournemouth University, Dorset, UK. *This author takes responsibility for all aspects of the*
16 *reliability and freedom from bias of the data presented and their discussed interpretation*
17
18

19
20 ²Department of Cardiology, Sunshine Coast Hospital and Health Services, University of the Sunshine Coast and
21 University of Queensland, Queensland, Australia. *This author takes responsibility for all aspects of the reliability*
22 *and freedom from bias of the data presented and their discussed interpretation*
23
24

25
26 ³Department of Intensive Care, Sunshine Coast Hospital and Health Services and University of Queensland,
27 Queensland, Australia. *This author takes responsibility for all aspects of the reliability and freedom from bias of*
28 *the data presented and their discussed interpretation*
29
30

31
32 ⁴Department of Cardiology, Poole Hospital NHS Foundation Trust, Centre for Postgraduate Medical Research
33 and Education, Bournemouth University, Dorset, UK. *This author takes responsibility for all aspects of the*
34 *reliability and freedom from bias of the data presented and their discussed interpretation*
35
36

37
38 ⁵Department of Cardiology, Poole Hospital NHS Foundation Trust, Centre for Postgraduate Medical Research
39 and Education, Bournemouth University, Dorset, UK. *This author takes responsibility for all aspects of the*
40 *reliability and freedom from bias of the data presented and their discussed interpretation*
41
42

43
44 ⁶Biomedical Research Unit, National Heart and Lung Institute, Imperial College, London, Royal Brompton
45 Hospital, London, UK. *This author takes responsibility for all aspects of the reliability and freedom from bias of*
46 *the data presented and their discussed interpretation*
47
48

49
50 ⁷Cardiovascular Science Research Centre, St George's Healthcare Trust, London, UK. *This author takes*
51 *responsibility for all aspects of the reliability and freedom from bias of the data presented and their discussed*
52 *interpretation*
53
54
55
56
57
58
59
60

61
62
63 ⁸Centre for Postgraduate Medical Research and Education, Bournemouth University, Dorset, UK. *This author*
64 *takes responsibility for all aspects of the reliability and freedom from bias of the data presented and their*
65 *discussed interpretation*
66
67

68
69 ⁹Centre for Postgraduate Medical Research and Education, Bournemouth University, Dorset, UK. *This author*
70 *takes responsibility for all aspects of the reliability and freedom from bias of the data presented and their*
71 *discussed interpretation*
72
73

74 ¹⁰Nutrition & Metabolism, Institute for Developmental Sciences, University of Southampton and Southampton
75 National Institute for Health Research Biomedical Research Centre, University Hospital Southampton,
76 Southampton General Hospital, Southampton, UK. *This author takes responsibility for all aspects of the*
77 *reliability and freedom from bias of the data presented and their discussed interpretation*
78
79

80
81 ¹¹Department of Cardiology, Sunshine Coast Hospital and Health Services, University of the Sunshine Coast and
82 University of Queensland, Queensland, Australia *This author takes responsibility for all aspects of the reliability*
83 *and freedom from bias of the data presented and their discussed interpretation*
84
85
86
87

88
89
90
91 **Correspondence author:**

92 Professor Kim Greaves

93 Department of Cardiology

94 Sunshine Coast Hospital and Health Services

95 Nambour 4565, Queensland, Australia.

96 Email: kim.greaves@health.qld.gov.au

97 Tel: +61 7 5370 3727

98 Fax: +61 7 5470 6084

99
100
101
102
103
104
105
106
107
108 **Grant support:** Bournemouth University PhD Scholarship, The Dorset Research Consortium and the Poole
109 Hospital Cardiology Research Fund

110
111 **Conflicts of interest:** None to declare

112
113
114 **Keywords:** Aortic valve calcification score, coronary microvascular dysfunction, calcific aortic valve disease.
115
116
117
118
119
120

121
122
123 **Abstract:**
124

125 **Background:** Although calcific aortic valve disease (CAVD) is associated with coronary atherosclerosis, it is not
126 known whether early CAVD is associated with coronary microcirculatory dysfunction (CMD). We sought to
127 investigate the relationship between myocardial blood flow reserve (MBFR) - a measure of CMD, and early
128 CAVD. We also determined whether this relationship was independent of coronary artery disease (CAD) and hs-
129 CRP, a marker of systemic inflammation.
130
131
132
133

134 **Methods:** 183 patients with chest pain and unobstructed coronary arteries were studied. Aortic valve
135 calcification score (AVCS), coronary total plaque length (TPL), and coronary calcium score were quantified from
136 multislice CT. MBFR was assessed using vasodilator myocardial contrast echocardiography. Hs-CRP was
137 measured from venous blood using a particle-enhanced immunoassay.
138
139
140
141

142 **Results:** Mean(\pm SD) participant age was 59.8(9.6) years. Mean AVCS was 68(258) AU, TPL was 15.6(22.2) mm,
143 and median coronary calcification score was 43.5AU. Mean MBFR was 2.20(0.52). Mean hs-CRP was 2.52(3.86)
144 mg/L. Multivariable linear regression modelling incorporating demographics, coronary plaque characteristics,
145 MBFR, and inflammatory markers, demonstrated that age ($\beta=0.05$, 95%CI:0.02,0.08, $P=0.007$), hs-CRP ($\beta=0.09$,
146 CI:0.02,0.16, $P=0.010$) and diabetes ($\beta=1.03$, CI:0.08,1.98, $P=0.033$), were positively associated with AVCS.
147
148
149
150
151
152
153
154
155
156
157
158
159
160
161
162
163
164
165
166
167
168
169
170
171
172
173
174
175
176
177
178
179
180

181 **Conclusion:** Coronary microvascular function as determined by measurement of myocardial blood flow reserve
182 is an independent predictor of early CAVD. This effect is independent of the presence of coronary artery
183 disease and also systemic inflammation.

181
182
183 **1. Introduction:**
184
185
186

187 The development of calcific aortic valve disease (CAVD) has traditionally been attributed to a passive, age-
188 related degenerative phenomenon. However recent evidence suggests a more active mechanism. CT coronary
189 angiographic studies have found an association between aortic valve calcification and the presence of coronary
190 artery disease, which is an inflammatory process (1, 2). Epidemiologic studies have identified that risk factors
191 for atherosclerosis - older age, male sex, hypercholesterolemia, hypertension, metabolic syndrome, and
192 smoking, are also independently associated with the presence of CAVD (3). Histopathological studies have also
193 observed the accumulation of atherosclerotic end products such as LDL, inflammatory cell infiltrates and
194 microscopic calcification, within explanted or cadaveric CAVD specimens (4). In addition, more recent findings
195 have shown that markers of inflammation such as hs-CRP, are independently associated with aortic valve
196 calcification (5). In the light of these and other findings, several groups have suggested that CAVD and coronary
197 atherosclerosis share common active pathophysiological mechanisms (6, 7).
198
199
200
201
202
203
204
205
206
207

208
209 The discovery of a link between both the early CAVD and coronary atherosclerosis has the potential to increase
210 understanding of the disease, improve risk stratification and provide therapeutic targets. Coronary
211 microvascular dysfunction (CMD) is a precursor to the development of coronary atherosclerosis (8). The
212 presence of CMD has been shown to predict the future development of coronary artery disease, and also
213 independently predict adverse cardiovascular and all-cause mortality. Therapies to improve CMD and outcome
214 have had some success (9-11). Whether or not CMD is independently associated with early CAVD is unknown.
215 Previous studies have attempted to examine whether there is a direct link between CMD and CAVD. However,
216 these have been limited to patients with established aortic stenosis which therefore represents late stage
217 CAVD, or assessed CAVD with echocardiography rather than CT (12, 13). Furthermore these studies either did
218 not exclude or quantify whether coronary artery disease was also present (14). This is important because even
219 the presence of mild non-obstructive coronary artery disease is known to be independently associated with
220 CMD and therefore a confounding factor (15)
221
222
223
224
225
226
227
228
229
230
231
232
233
234
235
236
237
238
239
240

241
242
243 We sought to investigate the relationship between myocardial blood flow reserve (MBFR) - a measure of CMD,
244
245 and early CAVD. We also determined whether this relationship was independent of coronary artery disease
246
247 (CAD) and hs-CRP, a marker of systemic inflammation.
248
249
250
251

252 **2. Methods:**

253
254
255
256 **2.1. Study population:** This pre-determined study was part of another study investigating the relationship
257
258 between chest pain typicality and its relationship to coronary microvascular function. This was a prospective,
259
260 cross-sectional, observational study which recruited consecutive patients aged 30-80 years attending
261
262 cardiology outpatient clinics (Jan 2011-March 2013) presenting with stable chest pain suggestive of myocardial
263
264 ischaemia due to CAD and who were referred for diagnostic CT coronary angiography (CTA). Those with
265
266 unobstructed coronary arteries underwent transthoracic echocardiography. Unobstructed CAD was defined as
267
268 a quantitatively measured luminal diameter stenosis <50%. Patients were excluded if they had ≥50% luminal
269
270 diameter narrowing, known ischemic heart disease, left ventricular hypertrophy, an ejection fraction <55%, or
271
272 significant aortic valve disease. Specifically, those patients with a peak systolic transaortic valve velocity of
273
274 >2m/s were excluded. Aortic valve calcification was quantified from the CTCA study. Participants then
275
276 underwent vasodilator myocardial contrast echocardiography (MCE) to assess myocardial blood flow reserve
277
278 (MBFR). Informed consent was obtained for each patient. The study complied with the Declaration of Helsinki
279
280 and was approved by the local research ethics committee (H0102/78).
281
282

283 **2.2. CTA study:** CTA imaging was performed using a 64-channel CT scanner (GE Lightspeed VCT, GE Medical
284
285 Systems, USA). The mean heart rate during the scan was 64 beats/min. A low dose scout scan was performed
286
287 to define anatomic landmarks for the contrast-enhanced study. Calcium scoring and helical scan data was
288
289 performed on all patients using prospective ECG triggering at 75% of the R-R interval. Following this, a 20ml
290
291 bolus of contrast (Niopram 370®) at 6mls/sec was injected and the timing of peak contrast enhancement in the
292
293 aortic arch was used to determine the timing of scan acquisition. The contrast-enhanced scan used 80mls
294
295 contrast injected at 6 ml/s, followed by a 50ml at 6mls/sec saline flush, during a single expiration breath hold.
296
297
298
299
300

301
302
303 The CTA scan parameters were: collimator 20mm, slice thickness 0.625mm; gantry rotation 350ms; helical
304 acquisition using a pitch of 0.16; tube current 455-515 mA with ECG tube current modulation; tube voltage
305 range 100-140kV; rotation time, 350ms. The estimated radiation dose per patient was 3.3mSv. Reconstructed
306 CTA images were analysed on a dedicated 3-dimensional workstation (CardIQ Xpress, GE Medical Systems) with
307 curved multiplanar reformation and short-axis cross sectional viewing techniques. We measured the amount of
308 plaque present in the proximal, mid, and part of the distal sections, of the main vessel coronary artery tree.
309 This decision was made because these segments have greater image quality regarding contrast:noise ratio,
310 reduced observer variability, and contain the majority of clinically important plaque in the coronary tree (16,
311 17). This included the left main stem (segment 1), the first 80mm of the left anterior descending (divided
312 equally into segments 2 and 3), the first 30mm of the circumflex (segment 4) and the first 80mm of the right
313 coronary artery (segments 5 and 6).

324
325 **2.3. Aortic Valve Calcification Score (AVCS):** Amount of aortic valve calcification is correlated with the degree
326 of aortic valve sclerosis applying multislice CT (18). For quantitative assessment of aortic valve calcification
327 using CT with a detection threshold of 130H, the aortic valve Agatston score was derived. Calcification was
328 attributed to the aortic valve if it was clearly part of the valve cusps. Supravalvular calcifications and
329 calcifications of the coronary arteries including the ostia were removed by manual segmentation. The Agatston
330 score was calculated by multiplying the lesion area by an attenuation factor derived from the maximal
331 Hounsfield units within the area, as previously described (19). Figure 1 illustrates this analysis.

332
333
334 **2.4. Coronary artery plaque burden:** Total plaque length (TPL) was used as a surrogate measure of total
335 atherosclerotic burden as described by Naya (20). Plaque length was measured as the distance (mm) from the
336 proximal to the distal shoulder of each plaque. TPL was calculated for each patient by summing all the lengths
337 for each subject. For each plaque, the degree of epicardial luminal narrowing was also assessed by quantifying
338 the percentage diameter stenosis. This was calculated by dividing the minimal lumen diameter at each plaque
339 by the nearest proximal normal artery diameter. The sum of all stenoses present divided by the number of
340 stenosed plaques, determined the total mean stenosis per patient.

361
362
363 **2.5. Coronary Calcium Score:** 2.5mm slice thickness, non-overlapping images were reconstructed using filtered
364
365 back projection and a standard algorithm (GE). The total calcium burden in the coronary arteries was manually
366
367 measured by planimetry according to the scoring algorithm of Agatston (19).
368
369
370
371

372 **2.6. MCE study:** Patients underwent the MCE study having avoided all caffeine-containing products in the
373
374 previous 24 hours. Patients withheld beta-blockers, nitrates and calcium antagonists the day before, and on
375
376 the day of the test. MCE was performed using a commercial ultrasound machine iE33 (Philips Medical Systems)
377
378 and SonoVue (Bracco Research SA) as the contrast agent given as a constant infusion. Real-time images were
379
380 recorded within 3-4 minutes in the apical 4-, 2- and 3-chamber views with low-power settings at a mechanical
381
382 index of 0.1. The focus was set at the mitral valve level. SonoVue was initially started at 60 mL/h through a
383
384 peripheral vein cannula with the VueJect infusion syringe pump (Bracco Research, SA), which gently rotates
385
386 and maintains the contrast agent in a suspension. Thereafter, the rate was set between 48 and 60 mL/h to
387
388 maximize image quality with minimal attenuation. Once optimized, the machine settings were held constant
389
390 throughout each participant study. Flash-impulse imaging at a high mechanical index (1.0) was performed to
391
392 achieve complete myocardial bubble destruction, after which 10 end-systolic frames were recorded digitally in
393
394 each apical view. After the resting images were acquired, dipyridamole was infused at 0.56 mg/kg over a 4-
395
396 minute period. After an interval of 2 minutes, post-stress images were recorded within 3 to 4 minutes. This
397
398 entire sequence took 14 minutes. Quantitative MCE analysis was performed offline using QLab V7.0 (Q-
399
400 Laboratory, Philips Medical Systems) as previously described in detail (21). Briefly, quantitative assessment of
401
402 myocardial perfusion was performed for 10 consecutive end-systolic frames after microbubble destruction. A
403
404 region of interest was placed over the thickness of the myocardium. Plots of peak myocardial contrast intensity
405
406 (representing myocardial blood volume A, dB) versus pulsing intervals (representing time) were automatically
407
408 constructed to fit the monoexponential function conventional equation: $y=A(1 - e^{-\beta t})$. From these plots, the
409
410 slope of the replenishment curve was determined (representing myocardial blood velocity β , dB/s). Figure 2
411
412 illustrates this analysis technique. The product of A and β yielded baseline MBF (dB²/s) and post-dipyridamole
413
414 MBF (stress MBF, dB²/s), respectively. We calculated MBFR by the ratio of stress MBF (MBFs) to baseline MBF
415
416 (MBFb). MBFR was calculated by dividing the MBFs by MBFb of the same segment. Basal segments were not
417
418 included in the analysis because of contrast attenuation. The remaining 10 mid- and apical cardiac segments
419
420

421
422
423 were analyzed. A segment was not included in the analysis if there was artifact, inadequate microbubble
424
425 destruction, attenuation, or a wide variation in contrast intensity to minimize errors.
426

427
428 **2.7. Venous samples:** Peripheral venous samples for hs-CRP were taken at rest. Fasting glucose and lipid
429
430 profiles were from within the previous 3 months. All assays were performed in duplicate by a single observer,
431
432 blinded to the demographic data. Hs-CRP was determined with a particle-enhanced immunoassay, which has a
433
434 detection limit of 0.1mg/L and an inter-assay CV <10% (Roche Diagnostics, UK).
435

436
437 **2.8. Statistical Analysis:** Where appropriate, continuous variables were summarised using means, standard
438
439 deviations and/or 95% confidence intervals. Ordinal and dichotomous variables were summarised using
440
441 proportions or percentages. Indices of variance are bracketed after the respective value for central tendency.
442
443 Normality was assessed using a Shapiro-Wilk test and if deemed necessary, heavily skewed data were
444
445 transformed using a natural logarithmic transformation. General correlation was checked using a Pearson's
446
447 correlation coefficient, and for categorical data, a Spearman's rank correlation (rho) test was employed.
448
449 Statistical significance was tested using either a Student t-test for normally distributed continuous data or a
450
451 Mann-Whitney U-test for non-normal continuous data. Ordinal and dichotomous data were tested using a
452
453 Fischer exact test. Univariate regression was used initially to quantify the relationships between each of the
454
455 explanatory variables and the main outcome variable MBFR against AVCS. Based on the results of the
456
457 univariate regression, multivariable model building was performed using ordinary least-square regression and
458
459 the resulting models were tested for coefficient (β) significance, model fit to data (adjusted R^2) and residual
460
461 homoscedasticity and normality. If required, a leverage to squared residual plot was used to assess the effects
462
463 of either high leverage or outlying values on the regression coefficients. A likelihood ratio (LR) test was
464
465 employed to compare the fit of each successive iteration to the regression model. The level of significance was
466
467 set at $P < 0.05$. For CTA studies, 10 patients' scans (60 segments) were re-analysed by KN, and then again by two
468
469 additional separate observers who were level 2 accredited or above (KG, RB). All analyses were performed
470
471 using STATA™ version 12.0.
472

473 **3. Results:**

474
475
476
477
478
479
480

481
482
483 Overall, our study included 183 participants whose baseline demographics are illustrated in Table 1. The mean
484
485 age of participants was 59.8(\pm 9.6) years of whom 52.5% were male with a mean BMI of 27.2(\pm 3.8) kg/m². The
486
487 mean hs-CRP was 2.52(\pm 3.86) mg/L, with 75 (41%) participants having elevated hs-CRP levels (defined as
488
489 >2mg/L).

492
493 **3.1. Aortic valve analysis:** In those with aortic valve calcification, the mean aortic valve calcification score
494
495 (AVCS) was 68(\pm 258) AU. In our cohort, the maximum AVCS was 2874 AU, and 72 (39%) had an AVCS of zero.
496
497 Due to the marked right skew present in AVCS, values were normalised using a natural logarithmic
498
499 transformation.

502
503 **3.2. Coronary artery plaque morphology:** From the 1096 segments available for analysis, 1016(92%) were
504
505 interpretable. The total coronary tree length studied was 190mm plus the mean left main stem length (8mm+
506
507 7mm). Plaque was present in 113(62%) of patients. There were 384 plaques in total and 53(29%) of patients
508
509 had either one or two plaques present. The mean stenosis per patient was 3.1(0-22)% of whom 138(76%) had a
510
511 mean stenosis of <5%. Values for total plaque length (TPL) were right skewed with a median (IQRs) of 19.3 (8.9,
512
513 31.7) mm. The mean TPL was 15.6 mm, ranging from 0 to 132 mm. When present, the median coronary
514
515 calcification score was 43.5(IQR 10.5-152) AU. Total coronary calcification score was also markedly right-
516
517 skewed. Inter and intra-observer variability (kappa) for both aortic valve and coronary calcium scoring was 0.85
518
519 and 1.0, respectively.

522
523 **3.3. Myocardial blood flow:** The mean MBFR was 2.20(\pm 0.52), and 70 patients (38%) had an MBFR below 2.0.
524
525 The intra- and inter-observer variability's for MBFR were 7.7% and 8.2%, respectively. The minimum number of
526
527 analysable segments for baseline and stress was six for each, in keeping with previous published data (22).

528
529 Table 2 shows the results of univariate analysis performed on all demographic parameters in addition to total
530
531 plaque length, coronary calcium score, hs-CRP and MBFR, in relation to aortic valve calcium score (AVCS). There
532
533 were significant positive correlations between increasing age, total plaque length, and hs-CRP with AVCS. There
534
535 was a significant negative correlation between MBFR, LDL and AVCS.

541
542
543
544
545 Multivariate model analysis incorporated all univariate parameters with a P value <0.20, each as independent
546 explanatory variables, using stepwise deletion from a fully saturated model. Each iteration was checked using a
547 likelihood ratio test against the fully saturated null model. No significant interaction terms were identified. The
548
549 final regression equation is demonstrated in figure 3.
550
551

552
553
554 The tabulated values for regression coefficients (β), 95% confidence intervals and P-values for each β , are listed
555 in Table 3. Age, diabetes, BMI, MBFR, LDL and hs-CRP are all independent predictors of AVCS. Coronary calcium
556 score and TPL were included separately during the model evolution due to strong collinearity and neither were
557
558 significant. As a result, the final model did not include either.
559
560
561

562
563
564 Figure 3 shows the regression model used to predict values for aortic valve calcification score. In the model,
565 increasing age, presence of diabetes, and hs-CRP are independent positive predictors of $\ln(\text{AVCS})$, whereas an
566 increased MBFR, BMI, and LDL are negatively associated with $\ln(\text{AVCS})$ ($R^2=0.36$). From the model, an absolute
567 change in the MBFR value by -1.0 results in an increase in AVCS by a multiple of 2.39AU.
568
569
570
571

572 573 574 575 **4. Discussion:** 576

577
578
579 Coronary microvascular function as determined by measurement of myocardial blood flow reserve is an
580 independent predictor of early CAVD. This effect is independent of the presence of coronary artery disease and
581 also systemic inflammation. Importantly, although coronary artery disease is initially associated with CAVD,
582 when MBFR is included in the model, coronary artery disease is no longer predictive.
583
584
585

586
587
588 **4.1. AVCS and microvascular function:** Previous studies have reported CMD in CAVD, however there are
589 several important differences with respect to our report. Banovic found that coronary flow reserve (CFR) using
590 Doppler echocardiography of the left anterior descending coronary artery, is reduced in asymptomatic but
591 haemodynamically significant moderate to severe AS with normal LV systolic function and unobstructed
592 epicardial coronary arteries (13). Importantly, they found that CFR was an independent predictor of mortality
593
594
595
596
597
598
599
600

601
602
603 after multivariate analysis even after taking into account haemodynamic indices of AS. They proposed that
604
605 lower CFR values in this context were caused by the upstream effects of haemodynamically significant AS, such
606
607 as left ventricular hypertrophy and fibrosis, with consequent reduced capillary density. Similarly, Rajappan
608
609 assessed CMD in patients with moderate to severe AS with unobstructed coronary arteries but used positron
610
611 emission tomography to measure CMD (12). They found that parameters of AS severity such as aortic valve
612
613 area and haemodynamic load were associated with CMD. Neither of these studies determined whether
614
615 coronary artery disease was present even if mild. This is important because even the presence of mild early
616
617 coronary artery disease is associated with CMD. For instance, Wang showed that increasing coronary calcium
618
619 score in asymptomatic individuals is associated with reduced coronary perfusion reserve (15). In fact,
620
621 endothelial dysfunction in the context of chest pain with unobstructed coronary arteries is a predictor of future
622
623 coronary atherosclerosis (23).

624
625
626 There is relatively limited data with regards to the relationship between early CAVD (without
627
628 haemodynamically significant AS) and CMD. Bozbas assessed CFR in patients with aortic valve calcification
629
630 without significant aortic stenosis. Aortic valve calcification was assessed using echocardiography (14). The
631
632 authors found that mean CFR was 16% lower in the AVC group compared to control ($p < 0.001$), and concluded
633
634 that CMD is present even during early CAVD. Multivariate analysis found that the presence of aortic valve
635
636 calcification was an independent predictor of CMD. However, although their patient cohort was asymptomatic,
637
638 they pointed out that their study had not excluded obstructive coronary artery disease.

639
640
641 Our study provides novel data for the following reasons. Firstly, early CAVD was diagnosed using CT, which is
642
643 more accurate than echocardiography in the assessment of aortic valve calcification (24). For example, one
644
645 group reported that CT had a greater sensitivity and detected 32% more patients than echocardiography in
646
647 their elderly screening cohort (24). The Agatston score for aortic valve calcification provides a much broader
648
649 range for quantitative scoring than the three point system used in Bozbas study. Finally, obstructive coronary
650
651 artery disease was excluded using CTCA whereas this was assumed from clinical history alone in previous
652
653 studies.

661
662
663 The role of microvascular dysfunction in relation to the development of CAVD is not yet clear. CMD has been
664 shown to correlate closely with endothelial dysfunction (25) and peripheral endothelial dysfunction assessed
665 using flow-mediated dilatation is also associated with aortic valve sclerosis. Therefore, when taken in
666 conjunction with our results, this suggests a systemic process (26). The recent discovery that valve endothelial
667 cells regulate the remodelling and integrity of the extracellular matrix within valve leaflets (27) may be
668 important. It has been proposed that endothelial dysfunction allows inflammatory cytokine entry into valve
669 leaflets which promotes mineralisation and ultimately leaflet calcification.
670
671
672
673
674
675
676
677

678 **4.2. AVCS and inflammation:** We found that the marker of systemic inflammation hs-CRP is independently
679 associated with aortic valve calcification score and is consistent with other published data (28). Oxidative stress
680 forms the initiating event of an inflammatory cascade which ultimately results in valvular calcification. Hs-CRP
681 correlates strongly with oxidative stress and studies are underway regarding its use as a surveillance biomarker
682 in the detection of atherosclerosis (5, 29). Furthermore, histopathology studies of explanted calcified aortic
683 valves have found an abundance of leucocytes and macrophages (4). Our findings add to the literature in that
684 CMD has a positive association with AVCS which is independent of and additive to the presence of systemic
685 inflammation.
686
687
688
689
690
691
692
693
694

695 **4.3. Other factors associated with early CAVD:** Our results indicated that Increasing age and presence of
696 diabetes were positively associated with AVCS. Neither of these findings are novel. The strong link between age
697 and valvular calcification is well established from epidemiology studies (3). Diabetes is a pro-inflammatory
698 condition which promotes macrophage deposition and consequent calcification (1).
699
700
701
702
703

704 Unexpectedly, in our analysis, increasing LDL was negatively associated with AVCS and is contrary to findings
705 from previous studies (30, 31). Low-density lipoproteins have been implicated in the pathogenesis of CAVD.
706 Extracellular lipid accumulation has been identified in explanted CAVD leaflets within the subendothelial layer
707 with apolipoproteins, implying a plasma source (32). However, the role of LDL in the early stages of CAVD
708 development is unknown especially given the failure of statin trials to slow AS progression (33). Importantly
709 36% of this patient cohort were on statin therapy prior to recruitment, and therefore a proportion of the study
710 population may have a history of chronically elevated LDL. Furthermore, recent reports have suggested that
711
712
713
714
715
716
717
718
719
720

721
722
723 lipid components other than LDL may be associated with AS progression and cardiovascular risk such as
724
725 lipoprotein(a) (Lpa) and non-HDL, (34, 35).
726
727

728
729 Increasing BMI was negatively associated with AVCS in our analysis. This was unexpected as a high BMI is
730
731 associated with both microvascular dysfunction and elevated systemic markers of inflammation, which
732
733 promote calcification (36, 37). However, observational data showing increased survival rates in higher BMI
734
735 patients presenting with acute coronary syndromes: the so-called obesity paradox, draws consideration of
736
737 whether higher BMI confers protection against certain disease processes (38).
738

739
740 **4.4. Study Limitations:** The study was conducted at a single centre in the UK which means referral bias may
741
742 have affected our sample population. Furthermore our participants consisted of patients referred for the
743
744 investigation of chest pain, which is not representative of the general population. However, the recruitment of
745
746 this patient population enabled CT-based radiological investigation which otherwise would not have been
747
748 ethically possible, and is consistent with previous studies (2, 14).
749

750 751 752 753 **5. Conclusion:** 754

755
756
757 Coronary microvascular function as determined by measurement of myocardial blood flow reserve is an
758
759 independent predictor of early CAVD. This effect is independent of the presence of coronary artery disease and
760
761 also systemic inflammation. Importantly, although coronary artery disease is initially associated with CAVD,
762
763 when MBFR is included in the model, coronary artery disease is no longer predictive.
764
765
766
767
768
769
770
771
772
773
774
775
776
777
778
779
780

REFERENCES

1. Alman AC, Kinney GL, Tracy RP, Maahs DM, Hokanson JE, Rewers MJ, et al. Prospective association between inflammatory markers and progression of coronary artery calcification in adults with and without type 1 diabetes. *Diabetes Care*. 2013;36(7):1967-73.
2. Nasir K, Katz R, Al-Mallah M, Takasu J, Shavelle DM, Carr JJ, et al. Relationship of aortic valve calcification with coronary artery calcium severity: the Multi-Ethnic Study of Atherosclerosis (MESA). *J Cardiovasc Comput Tomogr*. 2010;4(1):41-6.
3. Otto CM, Lind BK, Kitzman DW, Gersh BJ, Siscovick DS. Association of aortic-valve sclerosis with cardiovascular mortality and morbidity in the elderly. *NEJM*. 1999;341(3):142-7.
4. Mathieu P, Boulanger MC. Basic mechanisms of calcific aortic valve disease. *Can J Cardiol*. 2014;30(9):982-93.
5. Jeevanantham V, Singh N, Izuora K, D'Souza JP, Hsi DH. Correlation of high sensitivity C-reactive protein and calcific aortic valve disease. *Mayo Clin Proc*. 2007;82(2):171-4.
6. Gingham C, Florian A, Beladan C, Iancu M, Calin A, Popescu BA, et al. Calcific aortic valve disease and aortic atherosclerosis--two faces of the same disease? *Rom J Intern Med*. 2009;47(4):319-29.
7. Dweck MR, Khaw HJ, Sng GK, Luo EL, Baird A, Williams MC, et al. Aortic stenosis, atherosclerosis, and skeletal bone: is there a common link with calcification and inflammation? *Eur Heart J*. 2013;34(21):1567-74.
8. Johnson NP, Gould KL. Clinical evaluation of a new concept: resting myocardial perfusion heterogeneity quantified by markovian analysis of PET identifies coronary microvascular dysfunction and early atherosclerosis in 1,034 subjects. *J Nucl Med*. 2005;46(9):1427-37.
9. Bagi Z, Feher A, Cassuto J. Microvascular responsiveness in obesity: implications for therapeutic intervention. *Br J Pharmacol*. 2012;165(3):544-60.
10. Samim A, Nugent L, Mehta PK, Shufelt C, Bairey Merz CN. Treatment of angina and microvascular coronary dysfunction. *Curr Treat Options Cardiovasc Med*. 2010;12(4):355-64.
11. Eshtehardi P, McDaniel MC, Dhawan SS, Binongo JN, Krishnan SK, Golub L, et al. Effect of intensive atorvastatin therapy on coronary atherosclerosis progression, composition, arterial remodeling, and microvascular function. *J Invasive Cardiol*. 2012;24(10):522-9.
12. Rajappan K, Rimoldi OE, Dutka DP, Ariff B, Pennell DJ, Sheridan DJ, et al. Mechanisms of coronary microcirculatory dysfunction in patients with aortic stenosis and angiographically normal coronary arteries. *Circulation*. 2002;105(4):470-6.
13. Banovic M, Bosiljka VT, Voin B, Milan P, Ivana N, Dejana P, et al. Prognostic value of coronary flow reserve in asymptomatic moderate or severe aortic stenosis with preserved ejection fraction and nonobstructed coronary arteries. *Echocardiography*. 2014;31(4):428-33.
14. Bozbas H, Pirat B, Yildirim A, Simsek V, Sade E, Eroglu S, et al. Coronary flow reserve is impaired in patients with aortic valve calcification. *Atherosclerosis*. 2008;197(2):846-52.
15. Wang L, Jerosch-Herold M, Jacobs Jr DR, Shahar E, Detrano R, Folsom AR. Coronary Artery Calcification and Myocardial Perfusion in Asymptomatic Adults: The MESA (Multi-Ethnic Study of Atherosclerosis). *JACC*. 2006;48(5):1018-26.
16. Ferencik M, Nomura CH, Maurovich-Horvat P, Hoffmann U, Pena AJ, Cury RC, et al. Quantitative parameters of image quality in 64-slice computed tomography angiography of the coronary arteries. *Eur J Radiol*. 2006;57(3):373-9.
17. Hoffmann H, Frieler K, Hamm B, Dewey M. Intra- and interobserver variability in detection and assessment of calcified and noncalcified coronary artery plaques using 64-slice computed tomography: variability in coronary plaque measurement using MSCT. *Int J Cardiovasc Imaging*. 2008;24(7):735-42.
18. Koos R, Mahnken AH, Sinha AM, Wildberger JE, Hoffmann R, Kuhl HP. Aortic valve calcification as a marker for aortic stenosis severity: assessment on 16-MDCT. *AJR Am J Roentgenol*. 2004;183(6):1813-8.
19. Agatston AS, Janowitz WR, Hildner FJ, Zusmer NR, Viamonte M, Jr., Detrano R. Quantification of coronary artery calcium using ultrafast computed tomography. *JACC*. 1990;15(4):827-32.
20. Naya M, Murthy VL, Blankstein R, Sitek A, Hainer J, Foster C, et al. Quantitative relationship between the extent and morphology of coronary atherosclerotic plaque and downstream myocardial perfusion. *JACC*. 2011;58(17):1807-16.
21. Wei K, Ragosta M, Thorpe J, Coggins M, Moos S, Kaul S. Noninvasive quantification of coronary blood flow reserve in humans using myocardial contrast echocardiography. *Circulation*. 2001;103(21):2560-5.
22. Rana O BC, Kerr D, Coppini D, Zouwail S, Senior R, Begley J, Walker JJ, Greaves K. Acute Hypoglycaemia Decreases Myocardial Blood Flow Reserve in Patients With Type 1 Diabetes Mellitus and in Healthy Humans. *Circulation*. 2011;124:1548-56.

- 841
842
843 23. Bugiardini R, Manfrini O, Pizzi C, Fontana F, Morgagni G. Endothelial Function Predicts Future
844 Development of Coronary Artery Disease: A Study of Women With Chest Pain and Normal Coronary
845 Angiograms. *Circulation*. 2004;109(21):2518-23.
- 846 24. Owens DS, Plehn JF, Sigurdsson S, Probstfield JL, Launer LJ, Eiriksdottir G, et al. The comparable utility
847 of computed tomography and echocardiography in the detection of early stage calcific aortic valve disease: an
848 AGES-REYKJAVIK investigation. *JACC*. 2010;55(10s1):A71.E668-A71.E.
- 849 25. Pellegrino T, Storto G, Filardi PP, Sorrentino AR, Silvestro A, Petretta M, et al. Relationship between
850 brachial artery flow-mediated dilation and coronary flow reserve in patients with peripheral artery disease. *J*
851 *Nucl Med*. 2005;46(12):1997-2002.
- 852 26. Poggianti E, Venneri L, Chubuchny V, Jambrik Z, Baroncini LA, Picano E. Aortic valve sclerosis is
853 associated with systemic endothelial dysfunction. *JACC*. 2003;41(1):136-41.
- 854 27. Gould ST, Srigunapalan S, Simmons CA, Anseth KS. Hemodynamic and cellular response feedback in
855 calcific aortic valve disease. *Circ Res*. 2013;113(2):186-97.
- 856 28. Towler DA. Oxidation, inflammation, and aortic valve calcification peroxide paves an osteogenic path.
857 *JACC*. 2008;52(10):851-4.
- 858 29. Ridker PM. High-sensitivity C-reactive protein: potential adjunct for global risk assessment in the
859 primary prevention of cardiovascular disease. *Circulation*. 2001;103(13):1813-8.
- 860 30. Rajamannan NM. Mechanisms of aortic valve calcification: the LDL-density-radius theory: a translation
861 from cell signaling to physiology. *Am J Physiol Heart Circ Physiol*. 2010;298(1):H5-H15.
- 862 31. Pohle K, Mäffert R, Ropers D, Moshage W, Stilianakis N, Daniel WG, et al. Progression of Aortic Valve
863 Calcification: Association With Coronary Atherosclerosis and Cardiovascular Risk Factors. *Circulation*.
864 2001;104(16):1927-32.
- 865 32. O'Brien KD, Reichenbach DD, Marcovina SM, Kuusisto J, Alpers CE, Otto CM. Apolipoproteins B, (a),
866 and E accumulate in the morphologically early lesion of 'degenerative' valvular aortic stenosis. *Arterioscler*
867 *Thromb Vasc Biol*. 1996;16(4):523-32.
- 868 33. Rossebø AB, Pedersen TR, Boman K, Brudi P, Chambers JB, Egstrup K, et al. Intensive Lipid Lowering
869 with Simvastatin and Ezetimibe in Aortic Stenosis. *NEJM*. 2008;359(13):1343-56.
- 870 34. Capoulade R, Chan KL, Yeang C, Mathieu P, Bosse Y, Dumesnil JG, et al. Oxidized Phospholipids,
871 Lipoprotein(a), and Progression of Calcific Aortic Valve Stenosis. *JACC*. 2015;66(11):1236-46.
- 872 35. Boekholdt S, Arsenault BJ, Mora S, et al. Association of ldl cholesterol, non-hdl cholesterol, and
873 apolipoprotein b levels with risk of cardiovascular events among patients treated with statins: A meta-analysis.
874 *JAMA*. 2012;307(12):1302-9.
- 875 36. Tona F, Serra R, Di Ascenzo L, Osto E, Scarda A, Fabris R, et al. Systemic inflammation is related to
876 coronary microvascular dysfunction in obese patients without obstructive coronary disease. *Nutr Metab*
877 *Cardiovasc Dis*. 2014;24(4):447-53.
- 878 37. Eroglu S, Sade LE, Bozbas H, Muderrisoglu H. Decreased coronary flow reserve in obese women. *Turk*
879 *Kardiyol Dern Ars*. 2009;37(6):391-6.
- 880 38. Niedziela J, Hudzik B, Niedziela N, Gasior M, Gierlotka M, Wasilewski J, et al. The obesity paradox in
881 acute coronary syndrome: a meta-analysis. *Eur J Epidemiol*. 2014;29(11):801-12.
- 882
883
884
885
886
887
888
889
890
891
892
893
894
895
896
897
898
899
900

901
902
903
904
905
906
907
908
909
910
911
912
913
914
915
916
917
918
919
920
921
922
923
924
925
926
927
928
929
930
931
932
933
934
935
936
937
938
939
940
941
942
943
944
945
946
947
948
949
950
951
952
953
954
955
956
957
958
959
960

Table 1: Baseline Demographics

	All patients (n=183)
Age in years; mean (SD)	59.8 (9.6)
Male sex (%)	96 (52.4)
Diabetes (%)	18 (10.0)
BMI (kg/m²) (SD)	27.2 (3.8)
Smoking History (%)	
Non smoker	100 (55)
Ex-smoker	64 (35)
Current smoker	19 (10)
Hypertensive (%)	71 (38.8)
Family history (%)	91 (49.7)
Statin use (%)	66 (36.0)

BMI: Body mass index

Table 2: Univariate regression modelling of demographic variables, lipid profile and inflammation markers, coronary plaque parameters and microvascular function against aortic valve calcium score.

	β	95% CI	P-value
Age (yrs)	+0.07	+0.03, +0.10	0.01
Male sex (Y/N)	+0.05	-0.61, +0.71	0.08
Diabetes (Y/N)	+1.08	-0.11, +2.06	0.07
BMI (kg/m²)	-0.02	-0.12, +0.07	0.63
Smoking category (Y/N)	+0.31	-0.15, +0.77	0.19
Hypertension (Y/N)	+0.63	-0.02, +1.28	0.06
Family history (Y/N)	-0.36	-1.02, +0.30	0.29
Statin use (Y/N)	+0.63	-0.05, +1.30	0.07
LDL (mmol/l)	-0.45	-0.75, -0.15	0.003
Triglyceride (mmol/l)	+0.004	-0.33, +0.34	0.98
Total plaque length (mm)	+0.02	+0.01, +0.03	0.04
Coronary calcium score (AU)	+0.001	+0.001, +0.002	0.05
hs-CRP (mg/L)	+0.09	+0.01, +0.17	0.02
MBFR	-0.80	-1.41, -0.19	0.01

BMI: Body mass index, LDL: low-density lipoprotein, hs-CRP: high sensitivity C-reactive protein, MBFR:

myocardial blood flow reserve

Table 3: Multivariate regression modelling for predicting aortic valve calcification score using age, presence of diabetes, BMI, myocardial blood flow reserve, LDL, and hs-CRP

Variable	β	95% CI	P-value
Age (yrs)	+0.05	+0.02, +0.08	0.007
Diabetes (Y/N)	+1.03	+0.08, +1.98	0.033
BMI (kg/m ²)	-0.11	-0.21, -0.01	0.033
MBFR	-0.87	-1.44, -0.30	0.003
LDL (mmol/l)	-0.32	-0.61, -0.03	0.029
hs-CRP (mg/L)	+0.09	+0.02, +0.16	0.010

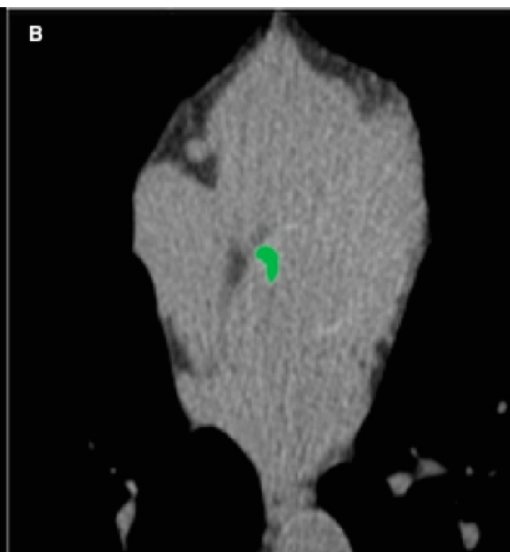
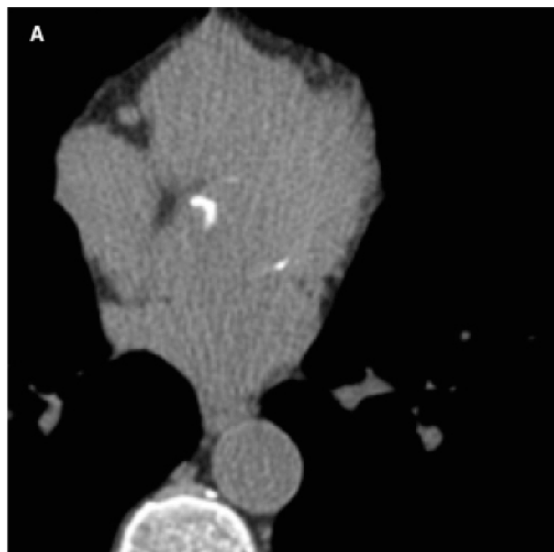
BMI: Body mass index, MBFR: Myocardial blood flow reserve, LDL: low-density lipoproteins, hs-CRP: high sensitivity C-reactive protein

1081
1082
1083 **Figure Captions:**
1084
1085
1086

1087 **Figure 1.** Example of aortic valve calcium scoring using ECG-gated coronary CT images. Calcification of aortic
1088 valve cusps detected on axial image (A). Imaging software detects regions within the aortic cusps with a density
1089 threshold of greater than 130HU to derive calcium volume (B). Aortic valve calcium score is then calculated -
1090 denoted in this case as 'U1' (C)
1091
1092
1093

1094
1095
1096 **Figure 2.** Model used for quantitative analysis of myocardial segments. (A) Apical 4 chamber, (B) Apical 2
1097 chamber, (C) Apical 3 chamber.
1098
1099
1100

1101
1102 **Figure 3.** Final model is described mathematically by $\ln(\text{AVCS}) = 5.83 + (0.05 \times \text{age}) + (1.03 \times \text{diabetes}) - (0.11 \times$
1103 $\text{BMI}) - (0.87 \times \text{MBFR}) - (0.32 \times \text{LDL}) + (0.09 \times \text{hs-CRP})$
1104
1105
1106
1107
1108
1109
1110
1111
1112
1113
1114
1115
1116
1117
1118
1119
1120
1121
1122
1123
1124
1125
1126
1127
1128
1129
1130
1131
1132
1133
1134
1135
1136
1137
1138
1139
1140



C

Artery	Lesions	Volume [mm ³]	Equiv. Mass [mg]	Score
LM	0	0.0	0.00	0.0
LAD	0	0.0	0.00	0.0
CX	0	0.0	0.00	0.0
RCA	0	0.0	0.00	0.0
TOTAL	0	0.0	0.00	0.0
U1	2	155.6	31.76	189.1
U2	0	0.0	0.00	0.0

Settings
Score Type: Agatston equivalent, Threshold: 130 HU (96.5 mg/cm² CaHA)
Mass calibration factor: 0.743

